

## Article

# Combined Physicochemical and Energy Methods to Improve the Recovery of Rare Earth Elements from Eudialyte Concentrate

Valentine A. Chanturiya, Vladimir G. Minenko , Andrey L. Samusev , Maria V. Ryazantseva \* and Elizaveta V. Koporulina

N.V. Melnikov's Institute of Comprehensive Exploitation of Mineral Resources Russian Academy of Sciences, Kryukovsky Tupik 4, 111020 Moscow, Russia

\* Correspondence: ryzanceva@mail.ru; Tel.: +7-(495)360-58-68

**Abstract:** The parameters for efficient nitric acid leaching were experimentally determined, which ensured the recoveries of Zr and REEs from eudialyte concentrate up to 87.0%–91.7% and 76.0%–81.1%, respectively. The possibility was shown of intensifying the leaching process through preliminary energy treatments to ensure the intensive breakdown of mineral complexes and grains; as a result, the recovery of Zr and REEs increased by more than 10%. A process was developed for the selective recovery of up to 91.5% of zirconium and up to 71.2% of REEs in the form of carbonate compounds from the pregnant solution of nitric acid leaching by chemical precipitation as well as up to 81.1% REEs and up to 91.7% zirconium on hypercrosslinked polystyrene sorbents.

**Keywords:** eudialyte; acid leaching; energy impacts; zirconium; rare earth elements



**Citation:** Chanturiya, V.A.; Minenko, V.G.; Samusev, A.L.; Ryazantseva, M.V.; Koporulina, E.V. Combined Physicochemical and Energy Methods to Improve the Recovery of Rare Earth Elements from Eudialyte Concentrate. *Minerals* **2023**, *13*, 414. <https://doi.org/10.3390/min13030414>

Academic Editors: Marinela Ivanova Panayotova and Vladko Panayotov

Received: 30 January 2023

Revised: 2 March 2023

Accepted: 10 March 2023

Published: 15 March 2023



**Copyright:** © 2023 by the authors. Licensee MDPI, Basel, Switzerland. This article is an open access article distributed under the terms and conditions of the Creative Commons Attribution (CC BY) license (<https://creativecommons.org/licenses/by/4.0/>).

## 1. Introduction

REEs are indispensable elements in the modern automotive, aerospace, metallurgical, chemical, electronic, energy and nuclear industries. It is impossible to produce high-tech communications, modern magnets, special steels, batteries, and computer chips without use of the REEs. In some sources, rare earth elements are called “metals of a new technological order [1]”.

However, the reserves of rich mineral resources (bastnasite, monazite, and xenotime) are limited, which is why there is a need for the development of new technology for processing the secondary REE resources. These resources include mineral feeds with a low content of REEs (apatites, eudialyte ores, and ocean bottom sediments) and waste (electronic scrap, phosphors, lighting bulbs, coal fly ash, etc.) [2–11].

A promising source of REE in Russia is the eudialyte ores (Lovozero deposit, Kola Peninsula). The resources of eudialyte ores of the Lovozero massif are huge (ZrO<sub>2</sub>: 300 million ton; REE oxides: 60–70 million tons). The content of the valuable components in eudialyte ores is quite low (0.5 g/t), but the content of the most valuable heavy REE (HREE) is sufficiently high (20%). Eudialyte is a potential source of Hf, and it usually contains very little thorium and uranium. This is why the development of technology for the recovery and separation of REE from the eudialyte is of current interest, taking into account the depletion of rich REE resources [12,13].

Various methods for the processing of eudialyte concentrates have been proposed in the literature [14–17]. The main problems of hydrometallurgical eudialyte processing is the formation silicic acid. It undergoes a polycondensation process with the formation of polymers of various compositions and structures up to stable gels. The latter leads to a drop in the recovery of valuable components. The various methods of silicic acid polymerization (silicate gel formation) are reported in the literature. Various solutions the silica gel formation problem have been proposed: silica gel formation can be avoided by applying a combination of mechanochemical and extraction with nitric acid/tri-n-butylphosphate [18],

the introduction of  $F^-$  ions during leaching [19], and a two-stage hydrometallurgical process [17], including preliminary acid treatment of the heated concentrate followed by aqueous leaching. In this paper, the use of energy effects on mineral pulp (ultrasound and electrochemical processing) is suggested. The experimental results show an increase in leaching efficiency and the opening of the silicate matrix [20,21].

Another significant problem with eudialyte processing is the recovery and separation of the valuable components (Zr and REE) from the pregnant solution of the eudialyte concentrate through leaching. However, the pregnant solution of the eudialyte concentrate leachate is quite complex in terms of the high concentration of the leaching agents, the low concentration of the valuable components, and the high concentration of the accompanying elements, most significantly alkaline earth. Extractive and sorption technologies are used for the selective recovery of the REEs from the leaching solutions. Among the human-made selective sorption materials, sorbents based on hypercrosslinked polystyrene are important [22]. The chemical inertness of hypercrosslinked polystyrene allows its use in aggressive media such as concentrated solutions of  $HNO_3$ ,  $HF$ , and  $H_2SO_4$ . The important advantage of this sorbent is the stability of the volume of the sorbent layer in the column during contact with electrolyte solutions of different concentrations; additionally, the method is simple and can be easily automated. It is also important that all used sorbents are produced on an industrial scale [23]. This paper presents the results of the application of sorbents based on hypercrosslinked polystyrene for the processing of a real pregnant solution of eudialyte acid leaching.

## 2. Materials and Methods

Eudialyte concentrate from the Lovozero field was used in leaching experiments (Table 1).

**Table 1.** Chemical composition of eudialyte concentrate (wt %).

Component	$Na_2O$	$MgO$	$Al_2O_3$	$SiO_2$	$K_2O$	$CaO$	$TiO_2$	MnO	$Fe_2O_3$
Content	10.14	0.18	6.90	44.96	1.37	5.42	3.29	1.66	5.20
Component	Cl	$SO_3$	$HfO_2$	$Nb_2O_5$	$Rb_2O$	$SrO$	<b>Ba</b>	U	Th
Content	0.97	0.20	0.14	0.81	0.01	2.63	0.09	<0.01	<0.02
Component	$ZrO_2$	$Ta_2O_5$	<b>As</b>	$CeO_2$	$Y_2O_3$	$Nd_2O_3$	$La_2O_3$	Other REE oxides	LOI
Content	11.50	0.05	0.03	0.68	0.46	0.32	0.29	0.75	1.97

Note: LOI, ignition loss.

Leaching conditions were varied depending on the aims of the experiments. These conditions are carefully detailed in [24,25] and are presented in Table 2.

**Table 2.** Leaching conditions.

Autoclave Name	Sample Mass, G	Acid Concentration, M	Temperature Range, °C	Residence Time, min	S:L Ratio	Agitation Speed, $min^{-1}$
TOP 120 series (TOP INDUSTRY)	60 g	2.4–9.6	80–140 °C	60–300	1:10	550
IPKON RAS Equipment *						

\* autoclave equipped with the fitting for US and EC treatment of mineral pulp during leaching.

Preliminary ultrasonic (US) treatment in water (5, 10, 20, and 30 min) and in a 7.2 M acid solution (10 min) was carried out with a dispersion machine (MEF-15, MELFIZ, manufacturer—MELFIZ, Moscow, Russia) at a power of 600 W and an operating frequency of 22 kHz at S:L = 1:10. Electrochemical (EC) treatment conditions were as follows: anode current density of 200 A/m<sup>2</sup> and volume current density of 1.5 A/L.

After the leaching, the insoluble mineral residue was separated from the pregnant solution with centrifugation (UC-1536 E, ULAB, China) then it was washed with distilled H<sub>2</sub>O and dried. The chemical composition of the solid residues was analyzed by ICP-MS (ICPE-9000, Shimadzu, Kyoto, Japan) after digestion with HNO<sub>3</sub> solution and XRF (ARL ADVANT'X, Thermo Scientific, Waltham, MA, USA). The chemical composition of the liquid phases was analyzed using ISP-AES (Elan-6100, PerkinElmer, Waltham, MA, USA) and MS.

The surface transformation of the eudialyte grains was examined with XPS (Versa Probe II spectrometer, ULVAC-PHI, Chigasaki, Japan) and DRIFT (IR-Affinity, Shimadzu, Kyoto, Japan).

The micromorphology and chemical composition of the eudialyte grains were determined using an analytical scanning electron microscope (ASEM) LEO 1420VP (Carl Zeiss, Cambridge, UK), equipped with an energy-dispersive X-ray INCA 350 spectrometer (Oxford Instruments Ltd., Oxford, UK) at an accelerating voltage of 20 kV in high-vacuum mode. The samples were fixed on a carbon conductive tape and coated with a thin layer of carbon.

Chemical precipitation of Zr and REE was performed in two steps. Zirconium hydroxides were recovered during the 1st step, when the leach solution was alkalinized with CaCO<sub>3</sub> to pH 3.8–4.0. The REEs were recovered during the second stage in the form of hydroxides and hydrocarbonates, with further solution alkalization with caustic soda (Na<sub>2</sub>CO<sub>3</sub>) to pH 6.0–6.4. Precipitates were separated from the solution. The final precipitates were washed with distilled H<sub>2</sub>O and dried to constant weight.

Highly crosslinked polystyrene sorbents DOWEX 1–X–8 (Acros Organics), PCA-433 (–1.2 + 0.3 mm), and Puomet MTS 9500, Purolite C 160 (Purolite) sized –63 + 43 μm were used in the study. The specifications of the sorbents used are presented in Table 3.

**Table 3.** Ion exchange resins used in the study.

Resin	Dowex 1 × 8 Strong Base Anion Exchange Resin Strongly Basic	Purolite PCA433 Strong Base Anion Exchange Resin	Purolite C160 Strong Acidic Exchange Resin	Puomet MTS 9500 Chelating Resin
Polymeric matrix	Styren divinylbenzene copolymer			
Functional group	Trimethyl ammonium	Quaternary ammonium type I	Sulfonic/aminophosphonic	Aminophosphonic
Exchange capacity	1.2 eq/L	1.3 eq/L	2.4 eq/L	1.3 eq/L Ca
Other properties	Gel polymer Crosslinking 8% Operating pH 0–14	Gel polymer Operating pH 0–14	Macroporous Operating pH 0–14	Macroporous chelating Operating pH 0–14

The preparation of polystyrene sorbents for the experiment was as follows: the sorbent sample was kept in a 50% HNO<sub>3</sub> solution for 24 h, then washed with distilled H<sub>2</sub>O until the neutral pH of the wash was reached.

In the sorption experiment, a pregnant acid leach solution was used (line 1 in Tables 4 and 5) as well as a refined REE solution obtained by dissolution (50% HNO<sub>3</sub>) of REE precipitate isolated from the initial pregnant solution during its neutralization with calcium carbonate, according to the method described above (line 2 in Tables 4 and 5).

The sorption experiment involved the following protocol: a 30 mL glass column was filled with water and sorbent granules, then a solution (1 mL/min) was fed through the column until the concentration of La at the column outlet was equal to the concentration at the column inlet. La was used as indicative element to control the column saturation with REEs as one of the representatives of the REE group.

After the column with the initial solution was equilibrated, the electrolyte was displaced by a top-to-bottom flow of the mobile phase. In both cases, the eluate was collected in 2.0 mL fractions, the content of metals in which was measured via ISP-MS, AES, and MS.

**Table 4.** Composition of the pregnant leach solution and refined REE solution.

	Na	Mg	Al	K	Ca	Ti	Si	Sc	Cr	Ni
	mg/L									
1	2272.0	16.1	520.7	115.7	1121.0	233.7	0.1	0.1	0.5	1.6
2	187.65	5.7	288.4	43.9	263.0	89.6	0.1	0.1	0.4	1.5
	Zn	Cu	Sr	Mn	Fe	Zr	Ba	Hf	Nb	ΣREE
1	13.6	0.8	580.0	527.0	580.0	2657.0	36.9	29.8	0.7	596.0
2	10.2	0.7	34.0	87.7	398.0	n/d	n/d	29.8	0.6	571.6

Note: n/d—not detected, below detection limits.

**Table 5.** REE concentration.

	Sc	Y	La	Ce	Pr	Nd	Sm	Eu	Gd	Tb	Dy	Ho	Er	Tm	Yb	Lu
	mg/L															
1	0.4	138.4	76.7	18.6	22.5	66.1	20.1	6.7	23.5	4.1	23.2	4.8	12.9	2.0	11.6	1.6
2	0.3	135.4	68.4	17.4	21.8	63.3	19.7	6.5	22.7	4.0	23.2	4.7	12.8	1.9	11.0	1.5

### 3. Results

#### 3.1. Effect of Acids on the Leaching Efficiency of Eudialyte Concentrate

**SPECIAL FEATURES OF EUDIALYTE SURFACE WHEN EXPOSED TO ACIDS.** The microscopic investigations revealed the morphological features of eudialyte particles after chemical interaction with acid solutions. We found that a main feature of the eudialyte particles after interaction with  $H_2SO_4$  and  $HCl$  solutions was the appearance of deep, vertical cracks (Figure 1b,c). It can be assumed that, in these acids, the mineral normal dissolution rate is comparable to and/or exceeds the tangential (layer-b-layer) rate, which contributes to a more active dissolution of the entire volume of the particle and not just its surface. A specific feature of the interaction of eudialyte with a  $HNO_3$  solution is the layer-by-layer mechanism of mineral dissolution (Figure 1a).

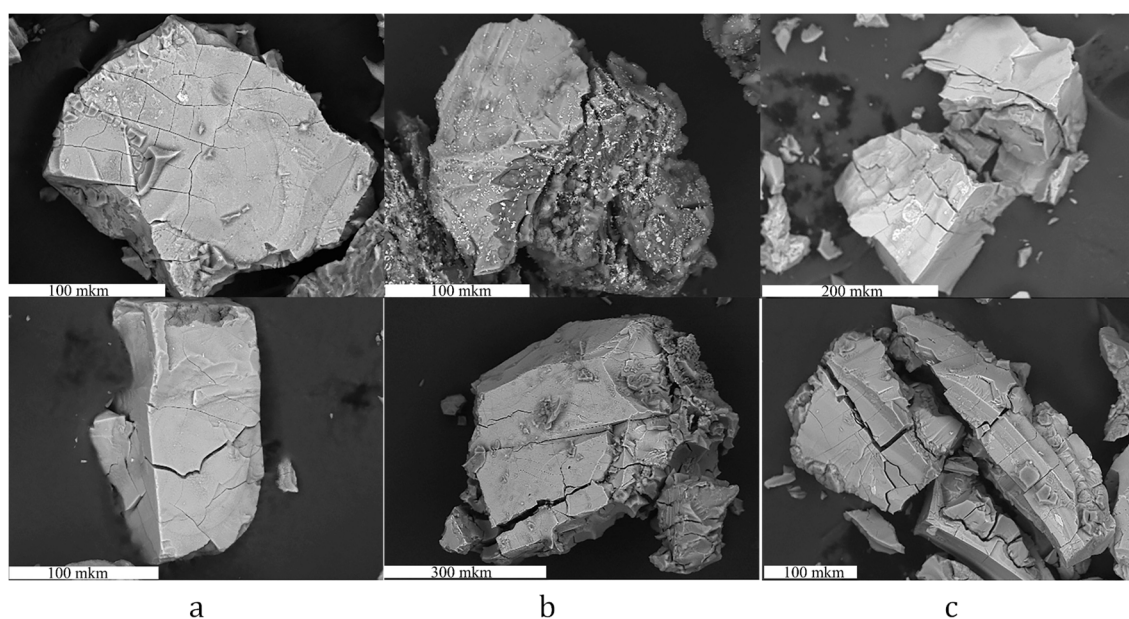


**Figure 1.** Different types of eudialyte grains transformation at tangential (layer-by-layer) dissolution in  $HNO_3$  (a) at the normal and tangential dissolution in  $H_2SO_4$  (b) due to the normal mechanism of dissolution in  $HCl$  (c).

Using the ASEM technique, it was determined that the degree of eudialyte grain destruction varied during the leaching process, while the grains of potassium feldspar, loparite, and aegirine were morphologically unchanged; the particles of lamprophyllite demonstrated the initial stage of dissolution.

Some secondary phases were found among the solid materials after the leaching of concentrate with  $\text{H}_2\text{SO}_4$ : the intergrowth of elongated gypsum and celestine crystals formed due to the interaction of  $\text{Ca}^{2+}$  and  $\text{Sr}^{2+}$  ions passing into the solution upon dissolution of lamprophyllite and the anionic group  $[\text{SO}_4]^{2-}$  (Figure 2).

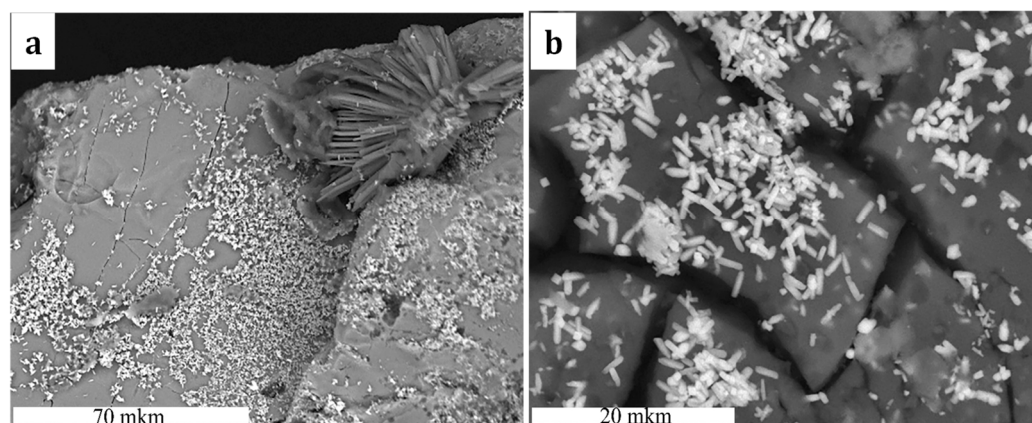


**Figure 2.** Secondary phases (celestine  $\text{SrSO}_4$  (a) and gypsum  $\text{CaSO}_4 \cdot 2\text{H}_2\text{O}$  (b)) in the residues of the leachate.

Most mineral particles after interaction with the  $\text{HNO}_3$  solution were considerably changed and covered with a dense layer of redeposited leaching products. The exception was individual grains of aegirine, which retained their initial needle-prismatic habitus. In addition, the formation of secondary phases was not excluded. Apparently, they were represented by a thin mixture of silicate gels with various degrees of hydration, with captured micron particles of acid-resistant minerals (egirine, loparite, feldspars), hydrolysis products of aluminum salts, as well as various ions of rare, alkaline, and alkaline earth elements sorbed from solution and complex ionic groups, presumably  $[\text{Nb}(\text{H}_2\text{O})_6](\text{OH})_2^{3+}$ ,  $[\text{Zr}(\text{NO}_3)_6]_2$ ,  $[\text{Zr}(\text{OH})_2]^{2+}$ ,  $[\text{NaSiO}_3]^-$ , etc.

The influence of various inorganic acids (hydrochloric, sulfuric, and nitric) on the eudialyte surface state was also studied by IR spectroscopy. The IR spectra of the sample both initially and after the interaction with  $\text{HCl}$ ,  $\text{H}_2\text{SO}_4$ , and  $\text{HNO}_3$  are given in Figure 3. The analysis of the obtained results led us to the following conclusion: the most considerable effect on the structural and chemical properties of the mineral was exerted by the  $\text{HCl}$  solution. Figure 3 shows that the spectra profile in the region from  $800\text{ cm}^{-1}$  to  $1350\text{ cm}^{-1}$  significantly changed compared with that of the initial (untreated) sample. For the sample after the interaction with  $\text{HCl}$  solution. A change in the band symmetry with an obvious broadening was observed: the shoulder at  $1135\text{ cm}^{-1}$  transformed into a distinct band at  $1145\text{ cm}^{-1}$ ; the peaks at  $980\text{ cm}^{-1}$  and  $1025\text{ cm}^{-1}$  disappeared.

A lowering of the mentioned band peak area was also observed. In the initial sample, the peak area value was about 585 rel. units, while for the sample treated with  $\text{HCl}$ , it was about 132 rel. units, i.e., a change by a factor of 4.4.

The action of the aqueous solutions of  $\text{H}_2\text{SO}_4$  and  $\text{HNO}_3$  on eudialyte modified its surface to a lesser extent. The spectra in the region of Si-O-Si bond-stretching vibrations maintained the symmetry; the area under the spectra in the discussed range dropped from 585 rel. units (initial sample) to 355 rel. units and 350 rel. units, respectively.

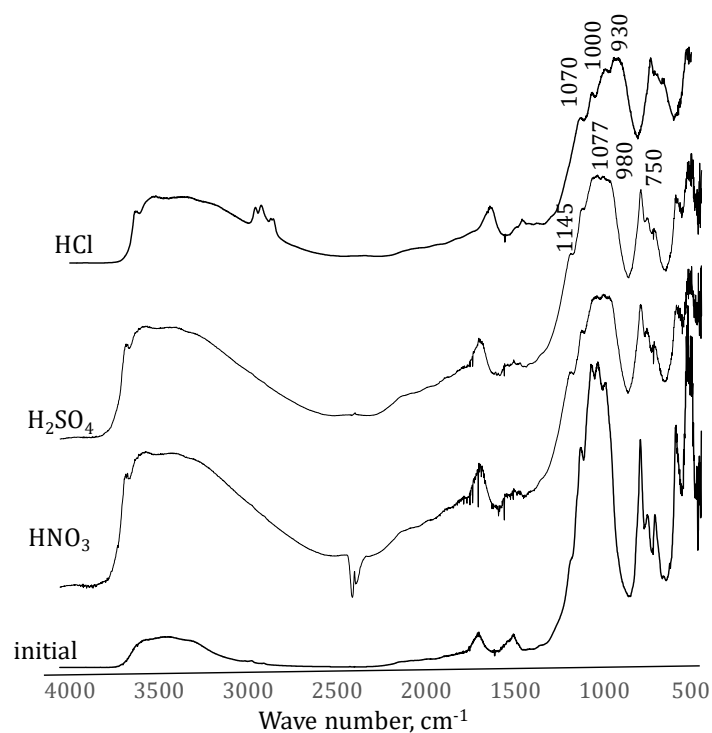


**Figure 3.** IR spectra of the initial eudialyte and of the sample after the interaction with HCl, H<sub>2</sub>SO<sub>4</sub>, and HNO<sub>3</sub>.

The XPS results generally agreed with the IR spectroscopy data. The results of the XPS study of the elemental composition (at.%) of eudialyte particles after the interaction with the solutions of HNO<sub>3</sub>, H<sub>2</sub>SO<sub>4</sub>, and HCl are presented in Table 6. The surface of the treated samples was depleted in metal content as a result of the intensive removal of cations from the surface into the leaching solution. The surface concentration of aluminum and sodium dropped by ~98%; calcium by 80%; magnesium, manganese, and potassium by 75%; titanium by 70%; and iron by 70%. The surface concentration of Si enhanced by 1.3–1.7 times.

**Table 6.** Atomic concentration (at.%) of eudialyte surface according to XPS data.

ACID	Atomic Concentration, at.%																ΣMe/Si
	C	N	O	S	F	Na	Mg	Ca	Al	Si	K	Ti	Mn	Fe	Sr	Zr	
No treatment	4.7	0.6	60.0	n.d.	0.6	12.2	0.5	0.5	2.8	14.8	0.4	0.9	0.5	0.7	0.4	1.2	1.36
HNO <sub>3</sub>	4.8	1.9	66.2	n.d.	0.1	3.4	0.2	0.2	1.4	19.2	0.2	0.6	0.2	0.5	0.2	1.2	0.42
H <sub>2</sub> SO <sub>4</sub>	2.5	0.3	69.2	2.2	<0.1	0.9	0.1	0.1	0.1	23.1	0.1	0.3	0.2	0.2	0.5	0.1	0.11
HCl	3.9	0.2	70.2	n.d.	0.1	0.2	<0.1	<0.1	<0.1	24.6	n.d.	0.1	<0.1	0.1	n.d.	0.4	0.05

Note: n.d.—not detected.

Through this process, the ratio of Me to Si significantly decreased, as shown in Table 6. The largest decrease in the Me/Si ratio was observed for the sample after the interaction with HCl (from 1.36 to 0.05), which confirmed that HCl was the most efficient agent for the leaching.

**LEACH CAKES.** The highest yield of metals from the eudialyte concentrate was observed when HCl was used as a leaching agent (Table 7). The ratio of ΣMe/Si in the cakes dropped by ~8 times (from ~1.7 to 0.2). When using the solutions of HNO<sub>3</sub> and H<sub>2</sub>SO<sub>4</sub> as the solvent, the obtained ratio of ΣMe to Si in the cakes was about 0.3.



and HCl, the recovery of Zr was 76% and 84%, respectively, and the  $\Sigma$  REE recovery was 79% and 83%, respectively (Table 8).

**Table 8.** Recovery of Zr and REE and losses with silicate gel under various leaching conditions and their concentrations in the pregnant solutions after the gel-like phase separation.

ACID	REE Recovery, %		Zr Recovery, %		Zr Loss with Gel, %	$\Sigma$ REE Loss with the Gel, %	$C_{Zr}$ in Pregnant Solution, g/dm <sup>3</sup>	$C_{REE}$ in Pregnant Solution, mg/dm <sup>3</sup>
	Gel	Solution	Gel	Solution				
H <sub>2</sub> SO <sub>4</sub>	70.22	12.34	26.90	64.65	30.0	85.0	4.50	221.6
HCl	18.76	64.74	8.34	75.57	10.0	23.0	5.00	999.3
HNO <sub>3</sub>	44.32	35.38	41.04	35.83	54.0	56.0	2.40	494.2
HNO <sub>3</sub> (US treatment)	29.39	54.52	29.39	57.87	32.25	35.03	3.10	637.1

However, sulfuric acid leaching provided the most significant losses of valuable components with gel-like silicate: the losses of Zr and  $\Sigma$  REE were about 30% and 85%, respectively, while in the HNO<sub>3</sub> and HCl solutions, the losses of Zr and REE were about 54% and 56%, and 10% and 23%, respectively (Table 8). At the same time, it should be noted that the US treatment of the mineral pulp produced an increase in the recovery and a drop in the loss of valuable components. The increase in the REE recovery was about 4% and the recovery of Zr rose to nearly 10% (Table 8) compared with those of the experiment without US treatment (Table 8). The reduction in the loss of Zr and REEs with the gel-like silicate was ~21% (from 54.0% to 32.25%).

Based on the above, in purified pregnant solutions (after removing the silicate gel), the maximum concentration of Zr and REE cations was observed with HCl leaching, at ~5.04 and 1.0 g/dm<sup>3</sup>, respectively (Table 8).

However, despite the good indicators of the leaching with the usage of HCl, this technology has no future in industrial processes for many practical reasons. This is why HNO<sub>3</sub> was chosen as the leaching agent in further studies.

### 3.2. Effect of Preliminary EC and US Treatments on the Nitric Acid Leaching

The utilization of various kinds of energy [20,26] is the alternative way of the hydrometallurgical process intensification. In this study, the effect of energy (US and EC) treatments and their combination on the efficiency of eudialyte concentrate leaching was examined.

EFFECT OF EC AND US TREATMENTS ON EUDIALYTE SURFACE EC treatment led to a significant reduction in the areas of particles covered by gel-like silica (Figure 6a,b) and to an increase in the areas composed of parallel teeth. The trigonal symmetry of the parallel-oriented teeth inherited the symmetry of the three- and nine-membered rings of silicon–oxygen tetrahedra located along the c axis of the eudialyte crystal structure. This indicated that leaching processes proceeded most intensively along this direction. The qualitative elemental composition of these regions was close to that of the original eudialyte, but the content of the rare earth elements significantly decreased and became below the detection limit of the energy-dispersive spectrometer.

The eudialyte particles after US treatment during the leaching demonstrated intensive surface fracturing until complete breakdown and the absence of silicate gel deposition (Figure 6c).

The results clearly demonstrated that the mineral surface layer was noticeably depleted in Al, Na, and Mg (% at.). The surface concentration of Al, Na, and Mg decreased by 2.0–4.5, 3.0–5.5, and 2.5–5.0 times, respectively. These data support the conclusion that the concentrations of Al, Na, and Mg in a sequence of studied samples consistently decreased. This shows that US treatment and its combination with EC treatment is more effective for breaking down eudialyte silicate matrices.

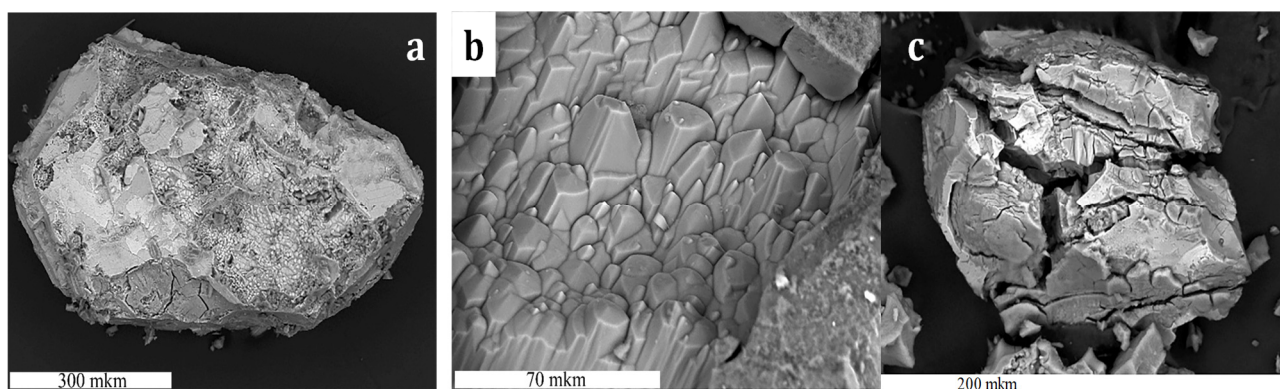


**Figure 6.** Surface of eudialyte grain (a) and area with serrate morphology (b) after leaching with EC treatment. Eudialyte grains after acid leaching with the application of US treatment (c).

Table 9 presents XPS results obtained for the initial (untreated) eudialyte sample and for the samples after the various treatments.

**Table 9.** XPS results of the eudialyte surface layer.

TREATMENT	Atomic Concentration, at. %													
	C	N	O	F	Na	Mg	Al	Si	K	Ti	Mn	Fe	Sr	Zr
1. None	4.7	0.6	60.0	0.6	12.2	0.5	2.8	14.8	0.4	0.9	0.5	0.7	0.4	1.2
2. HNO <sub>3</sub>	4.8	1.9	66.2	0.1	3.4	0.2	1.4	19.2	0.2	0.6	0.2	0.5	0.2	1.2
3. HNO <sub>3</sub> + EC treat.—200 A/m <sup>2</sup>	6.2	1.9	63.8	0.2	4.1	0.2	0.9	18.3	0.2	1.3	0.5	0.5	0.3	1.2
4. HNO <sub>3</sub> + EC treat. 200 A/m <sup>2</sup> + US 20 kHz	6.1	0.9	66.6	0.1	2.2	0.2	0.6	21.0	0.1	0.6	0.2	0.3	0.2	1.0
5. HNO <sub>3</sub> + US 20 kHz	4.9	1.2	67.7	0.2	2.4	0.1	0.7	20.2	0.1	0.7	0.2	0.5	0.1	1.1

The XPS and IR spectroscopy [24,25] data indicated that the eudialyte decomposition mechanism during the interaction with the leaching agent could be explained by the following processes: The first is associated with the selective extraction of alumina, sodium, and manganese. The second is associated with the breakdown of the silicate structure. At the same time, the concentration (at.%) of metal cations reduced, and the destruction of the silicate matrix was accompanied by the transformation of the silicate matrix into a gel-like phase. US and EC treatments significantly promoted the breakdown of the silicate matrix and improved the efficiency of eudialyte leaching.

### 3.3. Validation of the Optimized Process Modes and Process Flows for Nitric Acid Leaching of Eudialyte Concentrate

Special methods have been developed for identifying the dominant factors affecting various processes, which are called screening experiments. A mathematical model of a screening experiment with the preparation of a Plackett–Berman design was used in the study for the separation of the factors that insignificantly influenced the recovery of the valuable components with a minimum number of experiments, while ensuring the reliability of the results obtained (Table 10). The value of Zr recovery from the pregnant solution during the leaching of eudialyte concentrate was taken as a response. The influencing parameters ( $x_n$ ) were: ultrasonic treatment ( $x_1$ ), mineral pulp temperature in the leaching process ( $x_2$ ), the concentration of nitric acid ( $x_3$ ), electrochemical treatment ( $x_4$ ), and leaching duration ( $x_5$ ) (Table 10).

Table 10. Screening experiment plan.

Factor	US treat.	T, °C	C <sub>HNO<sub>3</sub></sub> , g/dm <sup>3</sup>	EC Treat.	t, h	Fictive Factors				y, %
Base level		60	450		2					
Variability interval		20	100		1					
Lower level (–)	no	40	350	no	1					
Higher level (+)	yes	80	550	yes	3					
code	x <sub>1</sub>	x <sub>2</sub>	x <sub>3</sub>	x <sub>4</sub>	x <sub>5</sub>	x <sub>6</sub>	x <sub>7</sub>	x <sub>8</sub>	x <sub>9</sub>	y
1	+	+	+	+	–	–	–	+	–	64.0
2	–	–	+	+	+	–	–	–	+	54.0
3	+	+	–	+	+	+	–	–	–	93.0
4	–	+	+	–	+	+	+	–	–	55.0
5	–	–	+	+	–	+	+	+	–	25.0
6	–	+	–	+	+	–	+	+	+	46.0
7	+	–	+	–	+	+	–	+	+	56.0
8	+	–	–	+	–	+	+	–	+	36.0
9	+	–	–	–	+	–	+	+	–	65.0
10	–	+	–	–	–	+	–	+	+	54.0
11	+	+	+	–	–	–	+	–	+	68.0
12	–	–	–	–	–	–	–	–	–	12.5
b <sub>i</sub>	11.29	10.96	1.29	0.62	9.12	0.79	–3.21	–0.71	–0.045	

The most valuable coefficients were determined:  $S_y^2 = 29.91$ ,  $S_{b_i}^2 = 2.8612$ , and  $\Delta_{b_i} = 4.702$ , from the results of the 12 experiments [27–30].

The analysis of the obtained results proved that the major parameters influencing recovery were US treatment, temperature of the pulp, and duration of the process.

The experimental studies of the influencing parameters were performed for the selection of the optimal parameters. The analysis of the obtained results showed that the correlation between the Zr recovery and US treatment followed a simple equation. The most significant values were achieved during the stable US treatment of the pulp. This experiment condition improved the Zr recovery by 2.8 times. This increase in the Zr recovery under the US treatment of the pulp could be explained by the fracturing of the eudialyte grains [27]. US treatment inhibited the formation of gel-like silica on the grains surfaces.

The results in Table 11 illustrate the influence of the leaching stage number (stage duration was 1 h) on Zr and REEs recovery. Two stages of the process increased the Zr recovery by approximately 10% and the REE recovery by 2%. In this case, the volume of gel-like silicate increased by 11% (from ~55% to ~66%), which led to increases in the Zr and REEs loss by ~10% and ~6%, respectively (Table 11, lines 1 and 3). A further increase in the number of stages from two to three led to the growth in the Zr recovery by 4.5% and in the REEs recovery by 2% (Table 11, lines 3–4). The total volume of gel-like silicate increased to 70% and, as a consequence, the loss of Zr and REE of with three stages of leaching was 60%.

The decreases in REEs and Zr losses with by the lowering of the duration of the first and second leaching stages with an increase in the duration of the third stage (while the total process duration was unchanged) were investigated. Reducing the durations of the first and second stages and the lengthening of the third-stage during provided gains in the Zr recovery by approximately 5% (Table 11, lines 4 and 5) and in REE recovery by 10% (Table 11, lines 4 and 5).

**Table 11.** Effect of the number and duration of leaching stages on the recovery of valuable components.

N	Acid/Treatment	n	t, min	$\epsilon, \%$		$\nu, \%$	
				Zr	REE	Zr	REE
1	HNO <sub>3</sub>	1	60	76.9	79.5	41	44.2
2	HNO <sub>3</sub> (US treatment)	1	60	87.3	83.5	32.3	35.0
3	HNO <sub>3</sub>	2	60/60	86.5	81.4	51.9	50.8
4	HNO <sub>3</sub>	3	60/60/60	91.1	83.2	60.3	59.9
5	HNO <sub>3</sub>	3	40/40/100	96.2	92.8	41.5	44.7
6	HNO <sub>3</sub> (1st-stage US treatment)	3	40/40/100	97.1	94.5	31.4	33.8
7	HNO <sub>3</sub> (H <sub>2</sub> SO <sub>4</sub> at 3rd stage)	3	40/40/100	95.8	91	41.5	44.7

Note: n—number of the stages; t—stage duration;  $\epsilon$ —recovery (total);  $\nu$ —loss of valuable component with gel.

At the same time, the volume of the gel-like silica insignificantly increased, while the loss of the valuable components was the same as that of the one-stage leaching process (Table 11, lines 1 and 5). The application of US treatment during the first leaching stage increased the total Zr and REEs recovery by 1% and approximately 1.5%, respectively (Table 11, lines 5 and 6), and reduced the volume of gel-like silica, which led to a drop in the loss of valuable components by 1.3 times.

The use of H<sub>2</sub>SO<sub>4</sub> acid during the third leaching stage had a little impact on the leaching efficiency: Zr and REEs recovery slightly dropped (Table 11, line 7).

Thus, a three-stage leaching process is recommended with the following conditions: duration of the first stage, 40 min, second stage, 40 min; and third stage, 100 min; nitric acid concentration, 450 g/L; mineral pulp temperature, 80 °C; S:L ratio, 1:20; continuous US treatment of the mineral pulp in the first stage of leaching. The application of the mentioned procedure enabled a Zr recovery of 97.1% and a REE recovery of 94.5%.

The technological scheme of eudialyte concentrate nitric acid leaching is depicted in Figure 7.

### 3.4. Recovery of Valuable Components from Pregnant Eudialyte Acid Leach Solution

#### 3.4.1. Recovery by Chemical Precipitation

The process of neutralizing the pregnant solution to pH 4.0 using calcium carbonate is accompanied by the chemical precipitation of zirconium and metal impurities [31,32]. The precipitate forms hydroxides (zirconium aluminum, and iron), carbonates, and hydroxides (REEs). The real solution has high mineralization, which is why the actual processes and chemical reactions may be more complicated than the theoretical reactions and require additional study.

Figure 8 a shows the dependence of the recoveries of Zr, Al, and Fe into a solid residue as a function of pH at 20 °C.

The efficiency of element precipitation increase with the rise in pH. At pH 4.0, the recovery of Zr and Al was about of 100% and that of Fe was 40%. At the same time, recovery of sodium, manganese, strontium, titan and potassium was 15–35% and REEs loss was ~9%. The sharp increase in REE loss up to 40.0 % (due to co-precipitation with zirconium) was observed during the further pH rising. At that time, the CaCO<sub>3</sub> consumption raised from 375 to 600 g/dm<sup>3</sup> due to the growth in solubility.

The separation of Zr and REEs must take place at pH 4.0–4.2 in order to achieve entire recovery of Zr, Al, and Fe. Further chemical precipitation of REE compounds should be carried out using Na<sub>2</sub>CO<sub>3</sub> and NaOH. The obtained results indicate the highest REEs recovery (96%) was achieved at a Na<sub>2</sub>CO<sub>3</sub> consumption of 6 g/dm<sup>3</sup> (pH 6.0). With NaOH application, the highest REEs recovery was 59%.

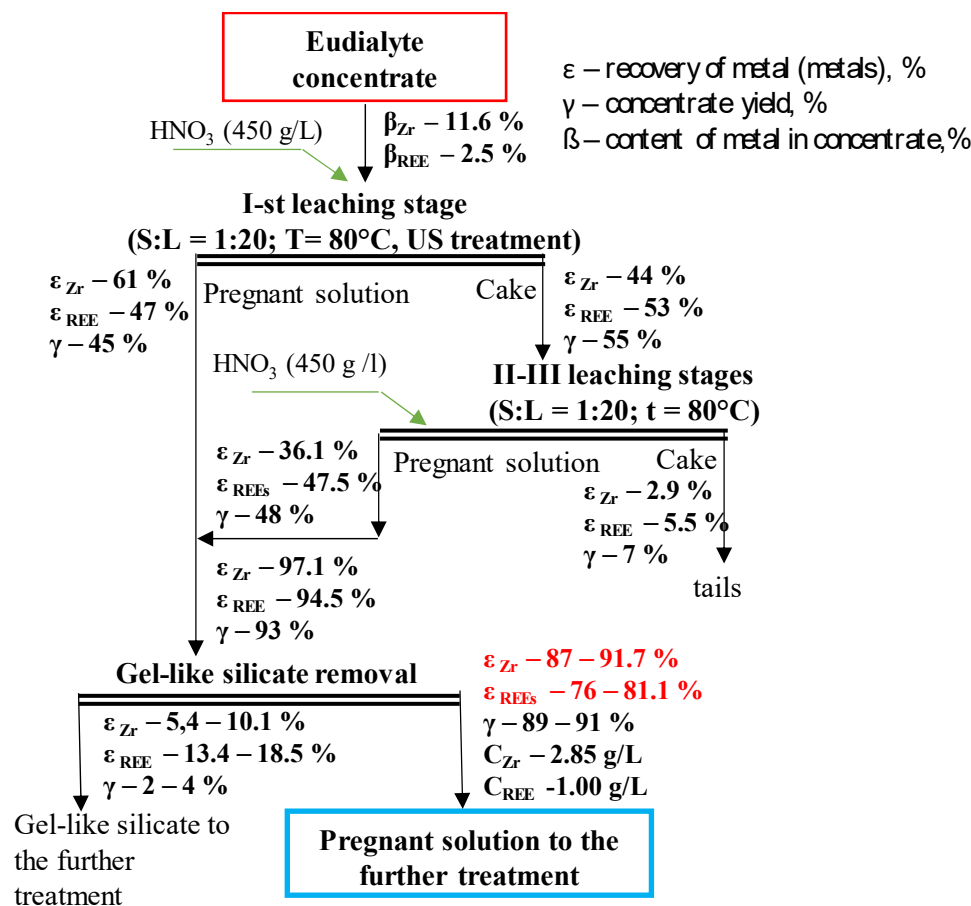


Figure 7. The developed scheme of eudialyte concentrate leaching.

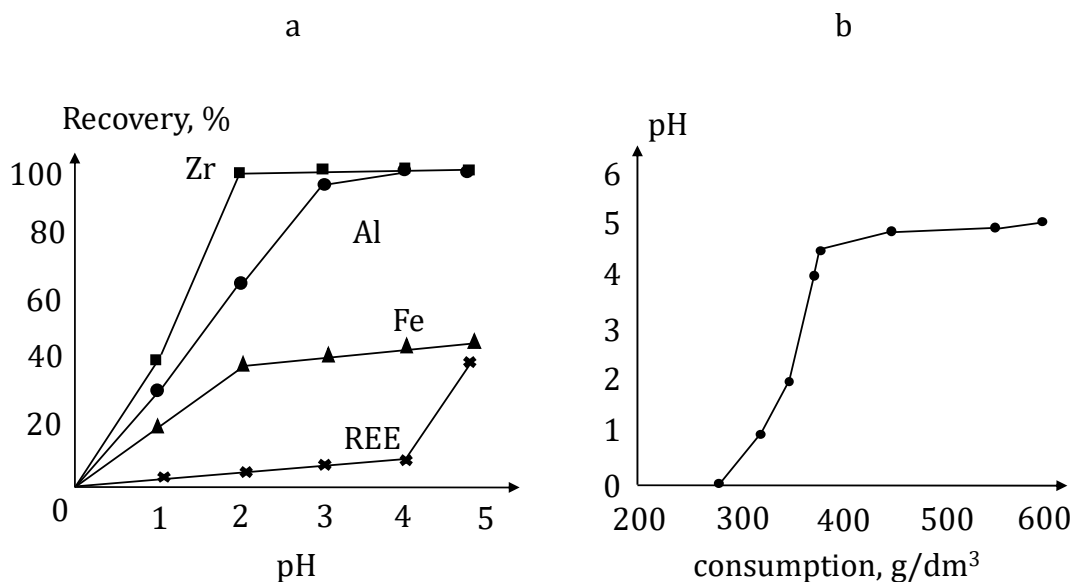


Figure 8. Effect of solution pH on elements' recovery into the solid precipitate (a), and the correlation of  $\text{CaCO}_3$  consumption and pH solution at 20 °C (b).

Small rounded particles were found among the main mass of solid precipitate. They contained rare earth elements of the cerium group (La, Ce, and Nd), yttrium, and synthetic hydroxyl analogs of bastnasite-group minerals: hydroxylbastnesite  $(\text{Ce, La, Y})\text{CO}_3(\text{OH, F})$  or hydroxylsynchysite  $\text{CaREE}(\text{CO}_3)_2\text{OH}$ . At the same time, we could not exclude the

deposition of aqueous rare earth carbonates calcinsite  $(\text{Ce, La})_2(\text{CO}_3)_3 \cdot 4\text{H}_2\text{O}$ , lanthanite  $(\text{Ce, La, Nd})_2(\text{CO}_3)_3 \cdot 8\text{H}_2\text{O}$ , or calcioanquilite  $\text{CeCa}(\text{CO}_3)_2(\text{OH}) \cdot \text{H}_2\text{O}$ . Because of the micron size of these particles, it was impossible to correctly determine their composition.

It was determined that the Zr recovery was independent of the initial concentration; it was 99.6%–99.9%. However, the increase in the initial REE concentration from 150 to 1200 mg/dm<sup>3</sup> led to increased loss with the residue from 0.3% to 8.5% due to the coprecipitation of rare earth elements with impurities [33,34].

#### 3.4.2. Sorption Method for the Recovery of REEs and Zirconium from Pregnant Eudialyte Acid Leach Solution

Three types of sorbents were used in this study: a strongly basic anion exchange resin (Dowex 1 × −8 and Purolite PCA 433), a strongly basic cation resin (Purolite C 160), and a chelate resin (Puromet MTS 9500). As expected, the two grades of highly basic anion resins produced very similar results. Although they differed somewhat due to the fact that Purolite PCA 433 carries a quaternary ammonium base as a functional group, which is known to have more pronounced basic properties than its tertiary forms. Figures 9 and 10 show the concentration curves obtained by the elution of a pregnant acid leach solution of eudialyte through the strongly basic polystyrene anion resins Purolite PCA 433 and Dowex 1 × −8.

The analysis of the obtained experimental data and the calculation of the material balance when using Purolite PCA 433 showed a sorption of 63.5% of  $\Sigma$  REE into the pregnant solution of the following elements: cerium (79.8%), lanthanum (67.5%), neodymium (99.5%), and praseodymium (81.1%) when eluate fractions 22 to 30 (0.88 to 1.20 of the column volume) were selected.

It was found that when eluting with water, the recovery of zirconium, lanthanum, cerium, and praseodymium from the resin was about 30%, 68%, 80%, and 20%, respectively. Thus, it was found that approximately 70% zirconium, 32% lanthanum, 20% cerium, and 80% praseodymium remained associated with the sorbent and could not be recovered in the reverse experiment (Table 12, column 1).

In order to desorb these elements, the sorption column was washed with 10 column volumes of the following solutions: 0.1 N and 0.5 N hydrochloric acid; 0.1 N, 0.5 N, and 8 N nitric acid; and 0.1 N sodium hydroxide at a flow rate of 1.0 mL/min. The results obtained are presented in Table 12, from which it can be seen that when washed with 0.1 N HNO<sub>3</sub>, the recovery of zirconium increased by 5.7% (from 29.9% to 35.6%); those of lanthanum, cerium, and praseodymium increased by 2.1%–2.3%.

Elution with 1 N HNO<sub>3</sub> was found to perform better and made it possible to increase the recovery of zirconium from 29.9% to 51.9%, i.e., by 22%. At the same time, the recovery of lanthanum increased from 67.5% to 72.5%, that of cerium from 79.8% to 85.4%, and that of praseodymium from 81.1% to 83.5%, which led to the total recovery of REEs increasing to 73.7%.

Under the same conditions, when passing the refined REE solution through the strongly basic anion resin Purolite PCA 433, the recovery of REEs increased to 75.3% ( $\Sigma$  REE content) in the initial solution (75.8% Ce, 80.6% La, 64.5% Pr, and 46.5% Nd) and to 59.5% Zr. When passing the initial pregnant solution through a strongly basic anion exchange resin Dowex 1 × −8 in a single pass, 61.3%  $\Sigma$  REE was extracted into the bulk selective fraction: cerium (84.1%), lanthanum (87.9%), neodymium (44.1%), and praseodymium (28.5%), when selecting eluate fractions 22 to 30 (0.88 to 1.20 of the column volume). As can be seen from the data presented in the Figure 9, it is important that when using DOWEX X 8, in contrast to PCA433, zirconium is recovered along with heavy REEs and alkaline earth metals in the first three-quarters of the column volume.

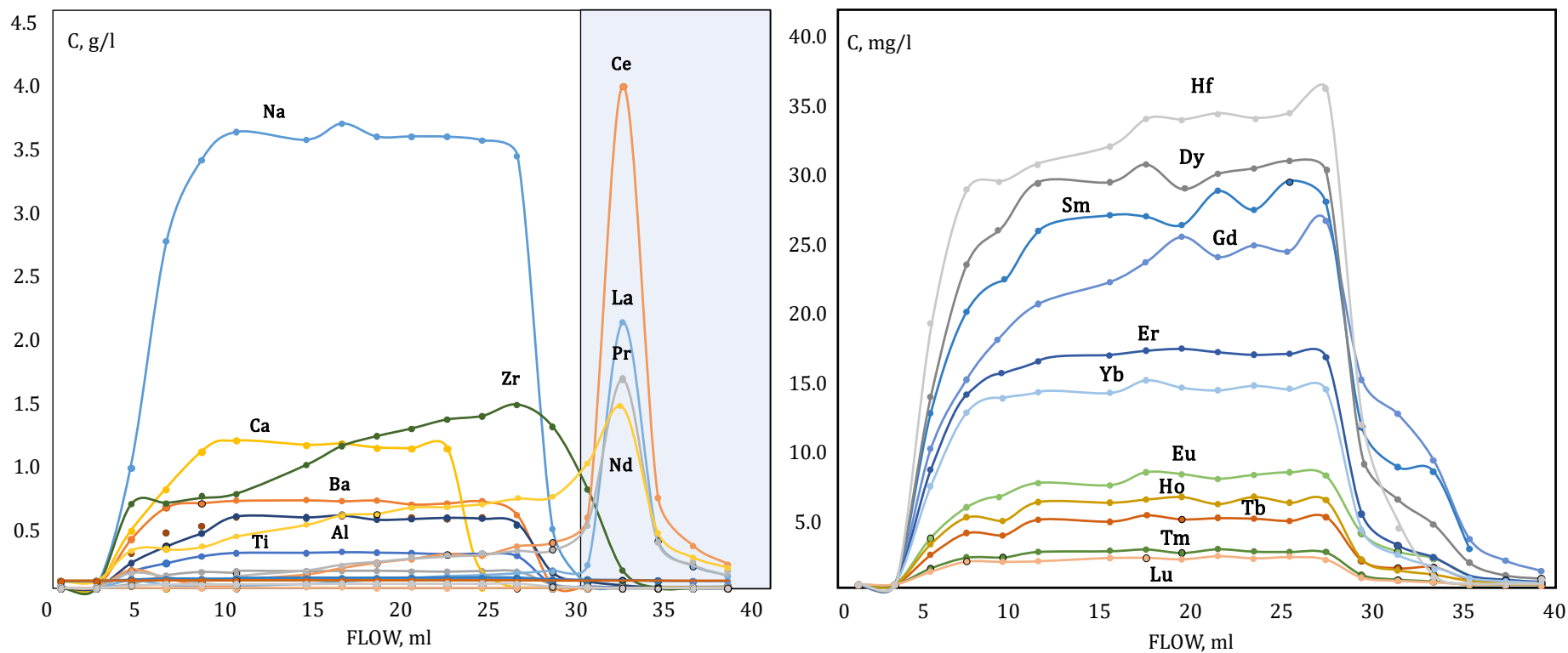


Figure 9. Pregnant solution elution curves through Dowex 1 × −8 sorbent.

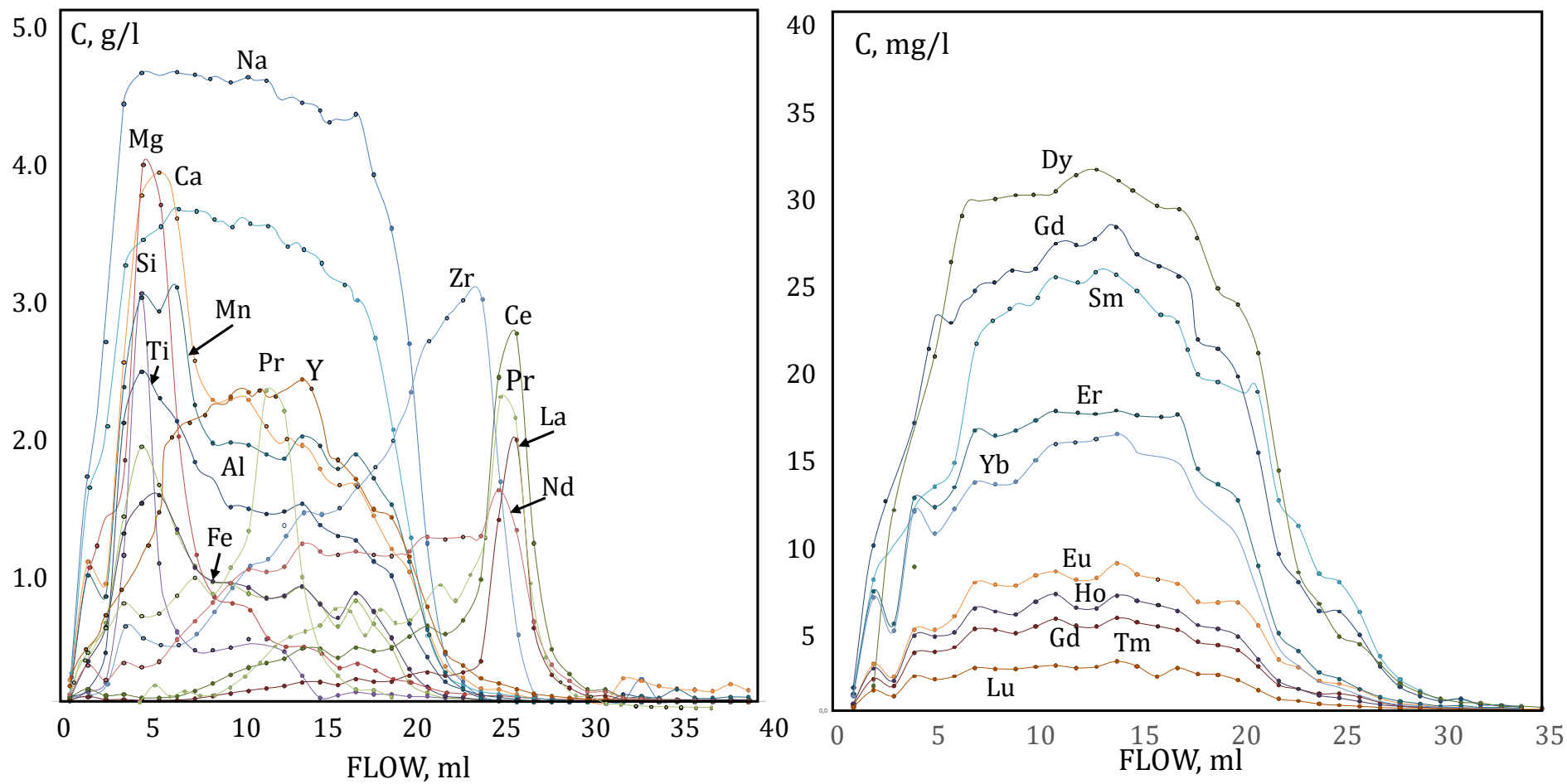


Figure 10. Refined REE solution elution curves through Purolite PCA-433.

**Table 12.** REE and Zr recovery with elution with various eluents.

	Recovery in H <sub>2</sub> O <sub>distill.</sub> , %	Recovery in 0.1 N HNO <sub>3</sub> , %	Recovery in 1.0 N HNO <sub>3</sub> , %
Zr	29.9	35.6	51.9
La	67.5	69.7	72.5
Ce	79.8	82.2	85.4
Pr	81.1	83.2	84.6
Nd	99.5	99.5	99.5

Passing a refined REE solution through a sorbent improved the process performance and made it possible to recover 70% of  $\Sigma$  REE in the solution in the bulk selective fraction due to an increase in the recovery of cerium by 1.1% (from 86.9 to 97.9), lanthanum by 9.1% (from 75.0 to 84.1), praseodymium by 9.3% (from 57.1% to 66.4%), and neodymium by 8.8% (from 35.3% to 44.1%), with additional recoveries of 28.5% of europium, 18.1% of samarium, and 35% of holmium and lutetium.

The analysis of the experimental data obtained for the strongly acidic cation exchanger Purolite C 160 and the chelate resin Puromet MTS 9500 revealed the priority of the sorption of total REEs. The recovery on the cation exchanger C 160 was 95% REEs, 83% Zr, 72% Sr, 80% Fe, 85% Mn, 83% Ca, 55% Al, and 67% Na. For the Puromet MTS 9500 sorbent, the recovery of total REEs and Zr into the resin was 99%; that of the associated elements ranged from 20% to 95% (Na 21%, Al 95%, Ca 28%, Mn 38%, Fe 95%, and Sr 17%).

Because the use of Puromet MTS 9500 made it possible to achieve higher recoveries of valuable components into the resin, while reducing the sorption of accompanying impurities, further research was aimed at finding effective desorbing agents (eluents) for the selective recovery of REEs and other sorbed elements.

During desorption, the feed method and feed rate of eluents were similar to those used in the process of feeding solutions to the sorbent; the volume of the passed desorption solution was 5–10 times resin volume (column volume). The list of desorption solutions is given in Table 13.

**Table 13.** Eluents and molarities.

Compound	Concentration, mol/L							
H <sub>2</sub> SO <sub>4</sub>	0.1	0.25	0.5	1.0	2.0	5.0	10.0	
HNO <sub>3</sub>	0.25	0.5	1.0	2.0	3.0	5.0	6.0	8.0
HCl	0.25	0.5	1.0	2.0	4.0	6.0		
NH <sub>4</sub> HF <sub>2</sub>	0.25	0.5	1.0	2.0	3.0	5.0		
EDTA	0.125 (pH 5.8)	0.125 (pH 4.5)	0.125 (pH 4.0)					
Citric acid	0.25	0.4	0.8	1.5	2.0			
Oxalic acid	0.20	0.4	0.8	1.5	2.0			

From our analysis of the experimental data (Figure 11) and calculation of the material balances, we drew the following histograms regarding the performance of the eluents used. Citric acid and EDTA showed poor performance in the process of desorption of the elements adsorbed by Puromet MTS 9500. The use of a 0.25 M solution of ammonium bifluoride (NH<sub>4</sub>HF<sub>2</sub>) made it possible to recover 98.9% of the zirconium, without any loss of REEs.

The use of 0.2 M oxalic acid as an eluate made it possible to recover 97.2% of the Na, while the concentration of rare earth elements in the eluate was below the detection threshold with the 0.05 ppm method, in other words, without the loss of REEs.

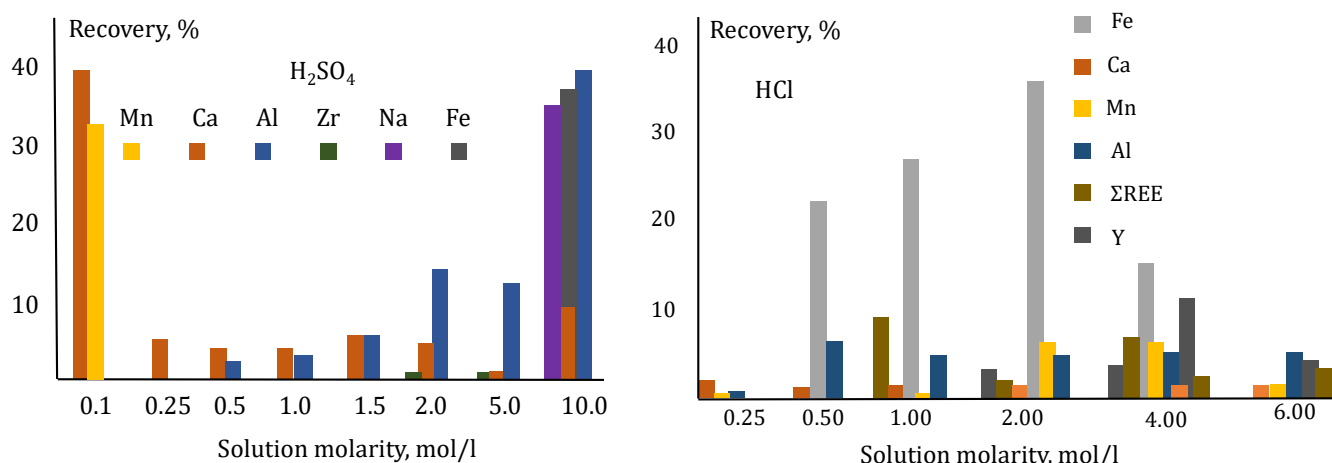


Figure 11. Recovery of the metals in sulfuric and hydrochloric acid (150 mL; %).

Sulfuric acid (H<sub>2</sub>SO<sub>4</sub>) at a concentration of 0.1 mol/L was an effective elution solution for Ca and Mn: when passing five column volumes (150 mL), 34% and 33% passed into the solution, respectively. Under the same conditions, sulfuric acid at a concentration of 10 mol/L caused the transition into the solution of 35% Na, 39% Ca, 37% Fe, and 38% Al. At the same time, the loss of REEs with the eluate of a 0.1 M H<sub>2</sub> SO<sub>4</sub> solution was 0.5% adsorbed on resin and 1.7% in the eluate of a 10 M solution (Figure 11).

Hydrochloric acid at concentrations of 0.5–2.0 mol/L, when passing five column volumes (150 mL), caused the transition to the elution solution of 22.54% to 36.3% Fe; at the same time, 2.31% to 9.29% of the REEs passed into the eluate (Figure 11b).

Finally, concentrated (5 and 8 M) solutions of nitric acid (HNO<sub>3</sub>) were found to be effective eluting agents for REEs. The 8 M solution performed better: when passing five column volumes, a recovery of 83.8% REEs was achieved; for 5 M, the recovery was 9.8% REEs. At the same time, 13.5% Al and 8.5% Ca passed into the 10 M nitric acid. The composition and concentration of REEs in the final product of REE desorption are shown in Table 14.

Table 14. REE concentration in the effluent (8 M HNO<sub>3</sub>).

La	Ce	Pr	Nd	Sm	Eu	Gd	Tb	Dy	Ho	Er	Tm	Yb	Lu	ΣREE
mg/L														
90.54	218.03	26.88	78.33	24.20	7.99	27.85	5.04	28.14	5.87	15.77	2.39	13.57	1.92	715.4

Based on the data obtained, two processes for the selective recovery of Zr and REEs from pregnant solutions of eudialyte concentrate leaching were proposed: sorption and precipitation–sorption (Figure 12).

The sorption extraction process involved feeding the pregnant solution in its native form to the Puromet MTS 9500 sorbent and the subsequent recovery from the sorbent by stepwise elution with mineral acid solutions (10–15 column volumes each, which ensured 100% removal of impurities), first of sodium; second of calcium, manganese, iron, and aluminum; third of REEs; and, finally, of zirconium into a solution of ammonium bifluoride.

The precipitation–sorption process involves sequential alkalization of the initial pregnant solution with calcium carbonate in order to isolate the zirconium product (pH 4) and REE carbonates with further introduction of sodium carbonate to pH 6.1. In order to remove impurities (Fe, Al, Ca, etc.), the resulting REE carbonates are proposed to be dissolved in 50% nitric acid and then REEs can be recovered into sorbents, followed by the selection of impurities and valuable REEs by elution with mineral acid solutions.

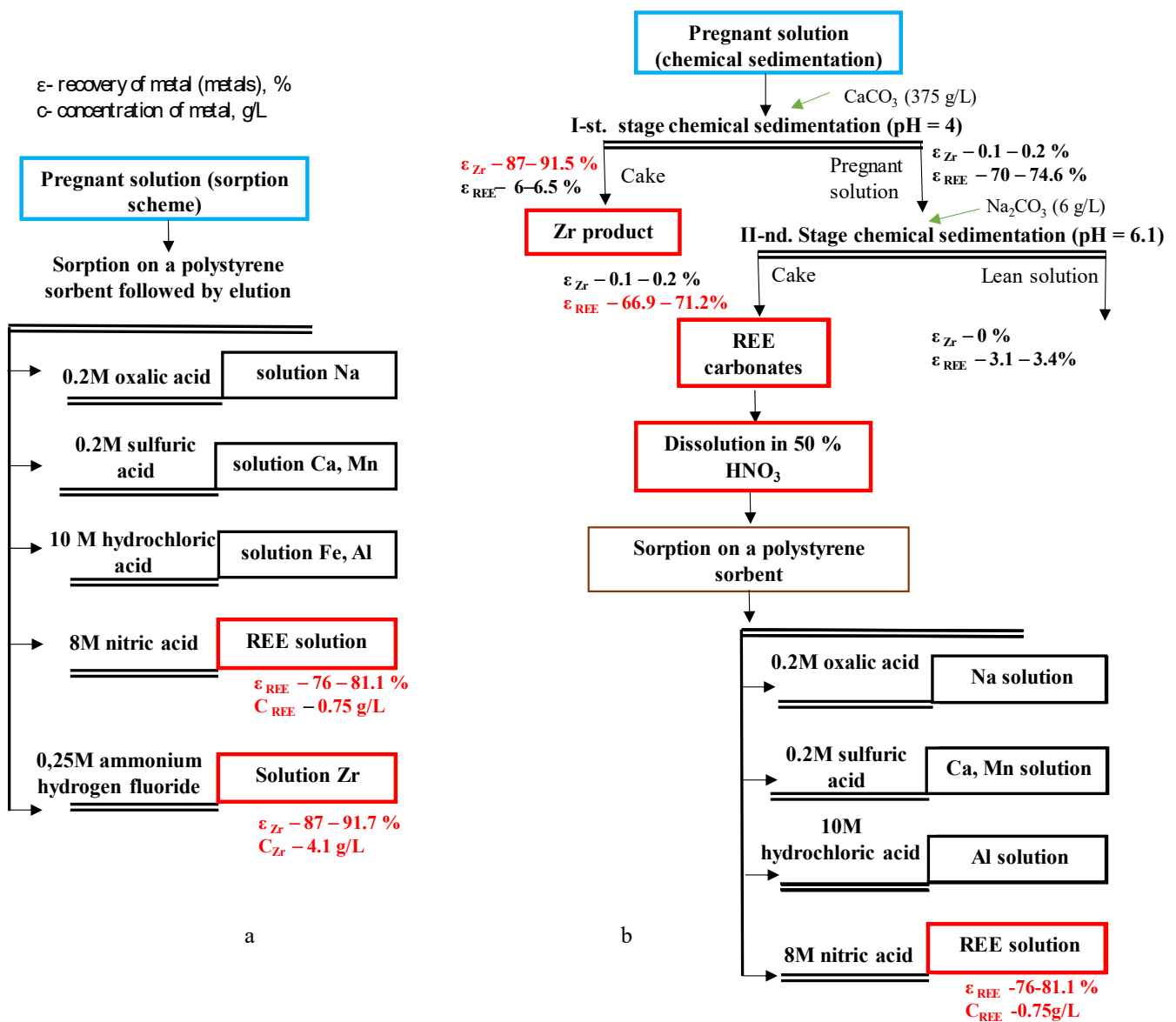


Figure 12. Schemes of the REE recovery from pregnant leaching solution through sorption (a) and precipitation-sorption schemes (b).

#### 4. Conclusions

The mechanism of the effect of various acids on the structural and chemical properties and dissolution of eudialyte concentrate was revealed. It was determined that during the interaction of eudialyte with HCl and H<sub>2</sub>SO<sub>4</sub>, the mineral surface is described by the appearance of a series of deep, parallel-oriented fractures because of the predominance of the normal dissolution rate. When interacting with HNO<sub>3</sub>, the tangential (layered) mechanism of dissolution dominates.

In the nitrogen-sulfuric-hydrochloric acid sequence, a consistent decrease in the content (at. %) on the eudialyte surface was identified for Al by 90%; Na by 98.4%; for Ca, Mg, and Mn by 75–80%; for Ti by 88%, and for Zr by approximately 92%. The phase composition of the silicate gel for all acids was characterized by Zr compounds, REEs, and nanofragments of the main concentrate minerals. According to the silicate gel formation efficiency and, accordingly, Zr and REE loss, the acids could be ranked as follows: sulfuric acid, nitric acid, and hydrochloric acid.

The most promising leaching results were obtained with HCl and HNO<sub>3</sub>, which provided comparable qualitative and quantitative process indicators. Because the applica-

tion of HCl is difficult because of many practical reasons, it cannot be recommended for industrial applications of the eudialyte concentrate leaching process.

The influence of combined energy treatment (thermal, electrochemical, and ultrasonic treatment) was determined. It consisted of dispersing the colloidal silicate gel, preventing the formation of its precipitates on the surface of mineral particles, and the formation of numerous defects and microcracks on the surface of eudialyte grains up to breakage during the ultrasonic treatment. It led to increases in the intensity and rate of the leaching process.

The greatest intensifying effect on the process of concentrate acid leaching was exerted by ultrasonic treatment of the mineral pulp. It enabled the highest Zr and REE recovery at a coarser feed size, lower slurry temperatures, and shorter leaching duration, as well as a reduction in REE loss to the gel by a factor of 2–2.5.

A highly efficient leaching process was developed for eudialyte concentrate, the practical implementation of which ensures a Zr recovery of 97.1% and a REE recovery of 94.5%, with significant reductions in silicate gel-like formation and valuable components loss by 21.0%, as well as increases in Zr and REE recovery by 10 % and 4%, respectively.

Our study demonstrated the high performance of Zr and REEs chemical precipitation. It was established that an increase in the pH of the initial pregnant solution during the first stage of precipitation with  $\text{CaCO}_3$  to 4.0 provided 99.95% Zr recovery into the solid phase and the associated recoveries of impurities: 100% of Al and 43.8% of Fe. The total recovery of REEs into the solid phase was as high as 74.6%, and the total loss of REEs with the product of the precipitation was 9%. A further increase in the pH of the solution using  $\text{Na}_2\text{CO}_3$  to 6.1 provided an REE recovery into the solid phase of 87.5%, with a total recovery from solution of 95.5%.

It was found that the use of the Puromet chelate resin MTS 9500 as a sorbent provided the highest (99%) recovery of REEs and Zr from the productive solutions. As a result of the subsequent stepwise gradient elution of the saturated sorbent, the following results were obtained: a Zr solution with a concentration of 4.1 g/L (Zr recovery into the solution was as high as 91.7%) and a REE solution with a concentration of 0.75 g/L (REE recovery 81.1%).

A process for the selective recovery of Zr and REEs from the pregnant leaching solutions of eudialyte concentrate based on a combination of chemical precipitation, sorption, and elution methods was proposed. Two process flows for treating pregnant solutions of eudialyte acid leaching were developed: sorption and precipitation–sorption.

**Author Contributions:** General scientific supervision of work V.A.C.; formulation of the research goals and aims, data analysis, and paper preparation; performing experiments (leaching), methodology development, IR, SEM, XPS results, data analysis, and preparation of the initial draft V.G.M., A.L.S., M.V.R. and E.V.K. All authors have read and agreed to the published version of the manuscript.

**Funding:** The research was carried out with the financial support of a project of the Russian Federation represented by the Ministry of Science and Higher Education of the Russian Federation No. 13.1902.21.0018 (agreement 075-15-2020-802).

**Data Availability Statement:** Not applicable.

**Acknowledgments:** Research was performed using the equipment of the NRC “Kurchatov Institute” Shared Knowledge Center.

**Conflicts of Interest:** The authors declare no conflict of interest.

## References

1. Vasilevskaya, D.V.; Saparov, S.M. *Mineral Resource Complex in the Period of Uncertainty and New Challenges: Results, Trends, Prospects*; Rusajns: Moscow, Russia, 2022; 130p.
2. Abaka-Wood, G.B.; Johnson, B.; Addai-Mensah, J.; Skinner, W. Recovery of Rare Earth Elements Minerals in Complex Low-Grade Sapolite Ore by Froth Flotation. *Minerals* **2022**, *12*, 1138. [[CrossRef](#)]
3. Jyothi, R.K.; Thenepalli, T.; Ahn, J.W.; Parhi, P.K.; Chung, K.W.; Lee, J.Y. Review of rare earth elements recovery from secondary resources for clean energy technologies: Grand opportunities to create wealth from waste. *J. Clean. Prod.* **2020**, *267*, 122048. [[CrossRef](#)]

4. Gaustad, G.; Williams, E.; Leader, A. Rare earth metals from secondary sources: Review of potential supply from waste and byproducts. *Resour. Conserv. Recycl.* **2021**, *167*, 105213. [\[CrossRef\]](#)
5. Abaka-Wood, G.B.; Addai-Mensah, J.; Skinner, W. The concentration of rare earth elements from coal fly ash. *J. South. Afr. Inst. Min. Metall.* **2022**, *122*, 21–28. [\[CrossRef\]](#)
6. Patil, A.B.; Tarik, M.; Struis, R.P.; Ludwig, C. Exploiting end-of-life lamps fluorescent powder e-waste as a secondary resource for critical rare earth metals. *Resour. Conserv. Recycl.* **2021**, *164*, 105153. [\[CrossRef\]](#)
7. Ait Brahim, J.; Ait Hak, S.; Achiou, B.; Boulif, R.; Beniazza, R.; Benhida, R. Kinetics and mechanisms of leaching of rare earth elements from secondary resources. *Miner. Eng.* **2022**, *177*, 107351. [\[CrossRef\]](#)
8. Binnemans, K.; Jones, P.T.; Blanpain, B.; Van Gerven, T.; Pontikes, Y. Towards zero-waste valorisation of rare-earth-containing industrial process residues: A critical review. *J. Clean. Prod.* **2015**, *99*, 17–38. [\[CrossRef\]](#)
9. Wang, N.; Sun, X.; Zhao, Q.; Yang, Y.; Wang, P. Leachability and adverse effects of coal fly ash: A review. *J. Hazard. Mater.* **2020**, *396*, 122725. [\[CrossRef\]](#)
10. Blissett, R.S.; Smalley, N.; Rowson, N.A. An investigation into six coal fly ashes from the United Kingdom and Poland to evaluate rare earth element content. *Fuel* **2014**, *119*, 236–239. [\[CrossRef\]](#)
11. Seredin, V.V. Rare earth element-bearing coals from the Russian Far East deposits. *Int. J. Coal Geol.* **1996**, *30*, 101–129. [\[CrossRef\]](#)
12. Savel'eva, I.L. The rare-earth metals industry of Russia: Present status, resource conditions of development. *Geogr. Nat. Resour.* **2011**, *32*, 65–71. [\[CrossRef\]](#)
13. Kuleshevich, L.V.; Dmitrieva, A.V. Rare-earth mineralization in Karelia's alkaline and moderately alkaline complexes, associated metasomatic rocks and ores. *Gorn. Zhurnal* **2019**, *3*, 45–50. [\[CrossRef\]](#)
14. Zakharov, V.I.; Skiba, G.S.; Solovyov, A.V.; Lebedev, V.N.; Mayorov, D.V. Some aspects of acid treatment of eudialyte. *TSvetnye Met.* **2011**, *11*, 25–29.
15. Lebedev, V.N. Sulfuric acid technology of eudialyte concentrate. *Russ. J. Appl. Chem.* **2003**, *76*, 1559–1563. [\[CrossRef\]](#)
16. Lebedev, V.N.; Shchur, T.E.; Maiorov, D.V.; Popova, L.A.; Serkova, R.P. Features of the acid decomposition of eudialyte and some rare metal concentrates the Kola Peninsula. *Russ. J. Appl. Chem.* **2003**, *76*, 1191–1196. [\[CrossRef\]](#)
17. Davris, P.; Stopic, S.; Balomenos, E.; Panias, D.; Paspaliaris, I.; Friedrich, B. Leaching of rare earth elements from eudialyte concentrate by suppressing silica gel formation. *Miner. Eng.* **2017**, *108*, 115–122. [\[CrossRef\]](#)
18. Chizhevskaya, S.V.; Chekmarev, A.M.; Klimenko, O.M.; Povetkina, M.V.; Sinegribova, O.A.; Cox, M. Non—Traditional methods of treating high—Silicon containing are elements. In Proceedings of the Hydrometallurgy'94, Cambridge, UK, 11–15 July 1994.
19. Dibrov, I.A.; Chirkst, D.E.; Litvinova, T.E. Experimental Study of Zirconium(IV) Extraction from Fluoride-Containing Acid Solutions. *Russ. J. Appl. Chem.* **2002**, *75*, 195–199. [\[CrossRef\]](#)
20. Chanturiya, V.A.; Chanturiya, E.L.; Minenko, V.G.; Samusev, A.L. Acid leaching process intensification for eudialyte concentrate based on energy effects. *Obogashchenie Rud* **2019**, 29–36. [\[CrossRef\]](#)
21. Chanturia, V.A.; Minenko, V.G.; Samusev, A.L.; Ryazantseva, M.V.; Koporulina, E.V. Influence Exerted by Ultrasound Processing on Efficiency of Leaching, Structural, Chemical, and Morphological Properties of Mineral Components in Eudialyte Concentrate. *J. Min. Sci.* **2018**, *54*, 285–291. [\[CrossRef\]](#)
22. Inamuddin; Luqman, M. (Eds.) *Ion Exchange Technology I: Theory and Materials*; Springer: Dordrecht, The Netherlands, 2012. [\[CrossRef\]](#)
23. Davankov, V.A.; Tsyurupa, M.P. *Hypercrosslinked Polymeric Networks and Adsorbing Materials, Synthesis, Structure, Properties and Application*; Elsevier: Amsterdam, The Netherlands, 2010; 648p.
24. Chanturia, V.A.; Minenko, V.G.; Koporulina, E.V.; Ryazantseva, M.V.; Samusev, A.L. Influence of Acids on Extraction Efficiency of Zirconium and Rare Earth Metals in Eudialyte Concentrate Leaching. *J. Min. Sci.* **2020**, *55*, 984–994. [\[CrossRef\]](#)
25. Chanturiya, V.A.; Minenko, V.G.; Samusev, A.L.; Chanturia, E.L.; Koporulina, E.V.; Bunin, I.; Ryazantseva, M.V. The Effect of Energy Impacts on the Acid Leaching of Eudialyte Concentrate. *Miner. Process. Extr. Metall. Rev.* **2020**, *42*, 484–495. [\[CrossRef\]](#)
26. Khokhlova, O.V. Povyshenie Effektivnosti Shchelochno-Kislotnogo Sposoba Kompleksnogo Vyshchelachivaniya Eudialitovogo Koncentrata. Ph.D. Thesis, University of Science and Technology (MISIS), Moscow, Russia, 30 May 2018.
27. Chanturia, V.A.; Minenko, V.G.; Samusev, A.L.; Chanturia, E.L.; Koporulina, E.V. The Mechanism of Influence Exerted by Integrated Energy Impacts on Intensified Leaching of Zirconium and Rare Earth Elements from Eudialyte Concentrate. *J. Min. Sci.* **2017**, *53*, 890–896. [\[CrossRef\]](#)
28. Durakovic, B. Design of Experiments Application, Concepts, Examples: State of the Art. *Period. Eng. Nat. Sci.* **2017**, *5*, 421–439. [\[CrossRef\]](#)
29. Jankovic, A.; Chaudhary, G.; Goia, F. Designing the Design of Experiments (DOE)—An Investigation on the Influence of Different Factorial Designs on the Characterization of Complex Systems. *Energy Build.* **2021**, *250*, 111298. [\[CrossRef\]](#)
30. Lee, B.C.Y.; Mahtab, M.S.; Neo, T.H.; Farooqi, I.H.; Khurshed, A. A Comprehensive Review of Design of Experiment (DOE) for Water and Wastewater Treatment Application—Key Concepts, Methodology and Contextualized Application. *J. Water Process Eng.* **2022**, *47*, 102673. [\[CrossRef\]](#)
31. Obrestad, T. Method for Producing Anhydrous Calcium Nitrate Powder. RU-2680036-C2 2680036C2, 14 February 2019.
32. Pozin, M.E. *Tekhnologiya Mineralnykh Soley*; Khimia: Leningrad, Russia, 1974; Part II.

33. Soltani, F.; Abdollahy, M.; Petersen, J.; Ram, R.; Becker, M.; Javad Koleini, S.M.; Moradkhani, D. Leaching and Recovery of Phosphate and Rare Earth Elements from an Iron-Rich Fluorapatite Concentrate: Part I: Direct Baking of the Concentrate. *Hydrometallurgy* **2018**, *177*, 66–78. [[CrossRef](#)]
34. Chen, S.; Huang, X.; Feng, Z.; Xu, Y.; Wang, M.; Xia, C.; Zhao, L. Behavior of Rare Earth, Iron, and Phosphorus during Purification of Rare Earth Sulfate Leach Solution Using Magnesium Oxide. *Hydrometallurgy* **2020**, *196*, 105377. [[CrossRef](#)]

**Disclaimer/Publisher's Note:** The statements, opinions and data contained in all publications are solely those of the individual author(s) and contributor(s) and not of MDPI and/or the editor(s). MDPI and/or the editor(s) disclaim responsibility for any injury to people or property resulting from any ideas, methods, instructions or products referred to in the content.